Materials Research Express

PAPER

Inkjet printed array antennas with frequency controlled beamsteering and multi-angle receiving

To cite this article: Peter Mack Grubb *et al* 2019 *Mater. Res. Express* **6** 046303

Materials Research Express

PAPER

Inkjet printed array antennas with frequency controlled beamsteering and multi-angle receiving

RECEIVED
22 November 2018

REVISED
2 December 2018

ACCEPTED FOR PUBLICATION
13 December 2018

PUBLISHED
9 January 2019

Peter Mack Grubb[1], Li Wentao[2] and Ray T Chen[1]

[1] Cockrell School of Engineering, University of Texas, Austin, United States of America
[2] Department of Electronic Engineering, Xidian University, Xi'an, People's Republic of China

E-mail: pmgrubb@utexas.edu

Keywords: frequency scanning array, flexible electronics, antenna array, printed silver

Abstract

This paper presents the first frequency scanning array on a flexible substrate constructed using printed electronics methods and systems. Devices were designed using a printed wide band stacked ellipsoid antenna and phase shifter network with 50 ohm matching power splitters which was developed using Ansys Electromagnetics. These devices were produced in both 1 × 4 and 1 × 8 antenna patch configurations. The resulting devices were then tested to demonstrate beam steering as a function of frequency at 4.35 GHz, 5.32 GHz, 6.27 GHz, and 7.2 GHz and compared. Additionally, bending tests were performed to demonstrate the usability of the devices in a flexible, internet of things oriented application. The demonstrated devices have a multibeam receiving and transmitting capability while being inexpensive and easy to produce in a flexible package.

1. Introduction

Printed electronics technology is one emerging manufacturing methodology which has seen significant growth in recent years. Of particular interest has been the ease and low cost with which printed electronics can fabricate flexible devices for usage in IoT applications [1]. This area of research has lead to significant work in designing various types of antennas optimized for printed electronics processes [2, 3]. One class of antennas that printed electronics methods are particularly well suited to are phased array antennas, which use phase shifter networks to create a controlled directional beam front. This is useful for communications applications, as it allows for tight beam communications to specific targets. However, the downside of a conventional phased array antenna is the need for switching between the various receiving angles, allowing the antenna to miss a signal from an angle it is not currently listening to, as well as the complicated fabrication inherent in variable phase shifter networks [4]. To this end, this paper proposes a design for a printed array based antenna which uses frequency as the scanning control element rather than phase shift. This allows for receiving from multiple angles using a microwave spectrum analyser, and negates the need for complex variable phase shifting elements.

Flexible inkjet printed antennas have seen significant development across multiple types of devices using differing materials and printing systems [2–6]. This paper will leverage the wide body of printing knowledge previously developed to demonstrate a new class of devices which have not been previously printed due to the challenges inherent in designing frequency scanning array systems on thin flexible substrates. The result is the first demonstration of a flexible, inkjet printed frequency scanning array.

Past efforts have successfully demonstrated that such a frequency scanning array would have continuous receiving across frequency bands supported by the antenna patches used to make up the design [7]. However, these efforts did not attempt to fabricate the devices, nor did they consider the potential performance under flex for these devices. Thus, this paper focuses on developing these theoretical structures into actual printed devices, and then demonstrating that their performance conforms to their simulated counterparts while extending the original results to show its capabilities specifically as a flexible device.

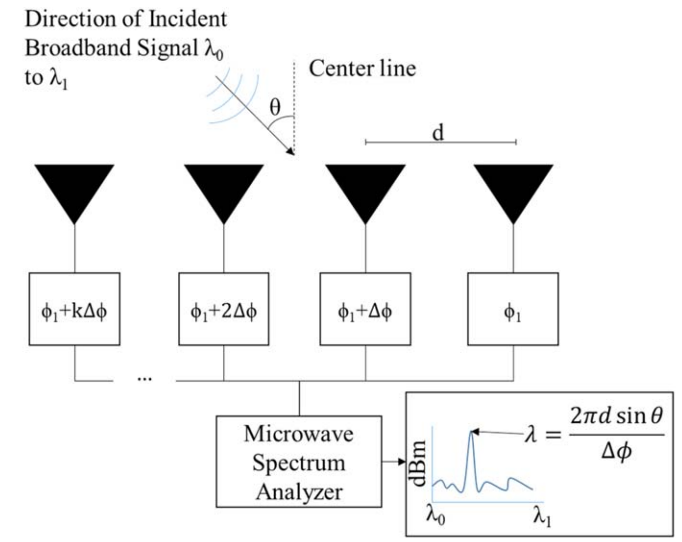

Figure 1. Due to the higher response on the MSA at λ, it can be concluded that the signal was received at an angle of θ from the center line.

2. Methods

2.1. Theory of frequency scanning arrays

Previous papers have clearly outlined the effects of frequency on the beam squint of frequency controlled phased array antennas, typically described as a 'Frequency Scanning Array' or FSA [8, 9]. However, these types of devices have not previously been constructed using printed electronics methodologies, nor have they been constructed on flexible substrates. Given the reliability of conductive printed electronics and the power budgets associated with the internet of things application, this type of antenna is uniquely suited to printing applications. To understand the operating principle, it is first important to understand the operating principle of a phased array antenna (PAA).

PAAs use a series of identical antennas connected to a phase shifter network, usually implemented using a time delay circuit [10]. The phase shifts generate a signal with a net directionality. The directionality of this signal is determined by the magnitude of the phase shift. Using the equations describing the N-slit diffraction phenomena, the relationship between these phase shifters and the angle of the directional signal can be derived to be $\Delta\phi = 2\pi\frac{d}{\lambda}\sin\theta$, where ϕ is the phase shift, d is the distance between the antennas, λ the wavelength and θ the direction of propagation [11]. This principle also applies to an antenna used as a receiver, though in this case the equation governs the direction of maximum sensitivity rather than the direction of transmission.

For a frequency scanning array, the phase shift is held constant. Instead, shifts in λ are used to achieve the directionality of the signal. This effect is illustrated in figure 1. The critical effect of this phenomena is that the array does not have to scan available angles, and can instead determine which direction a signal was received from purely by the wavelength of the strongest response, assuming that the transmitter has a similar bandwidth to the receiving antenna.

This principle also works for transmission. Signals can be sent in multiple specific directions simultaneously by running multiple different frequency signals into the array. This is similar in principle to the technologies used to have multiple simultaneous transmissions in a cable modem for residential internet [12].

2.2. Printed frequency scanning array design

One of the main design challenges regarding building a frequency scanning array on a flexible substrate is the relative thinness of the substrate. Typically substrate thickness is varied to improve properties such as gain or microstrip performance. However, the 5 mil/125 micron Kapton is the thickest option that Dupont currently sells [13]. Additionally, other flexible polymide films have much lower curing temperatures, rendering them incompatible with many silver ink compounds [14]. Consequently, the antenna system must be designed to accommodate the thin substrate being used.

The antenna system consists of three elements: the broadband antenna, the phase shifter network, and the input coupler, an example of which is illustrated in figure 2(A). For the input coupler, a simple SMA to microstrip transmission was used to allow for easy connection of various pieces of measurement equipment to the antenna system. The width of the base of the input coupler was determined by the SMA specifications for

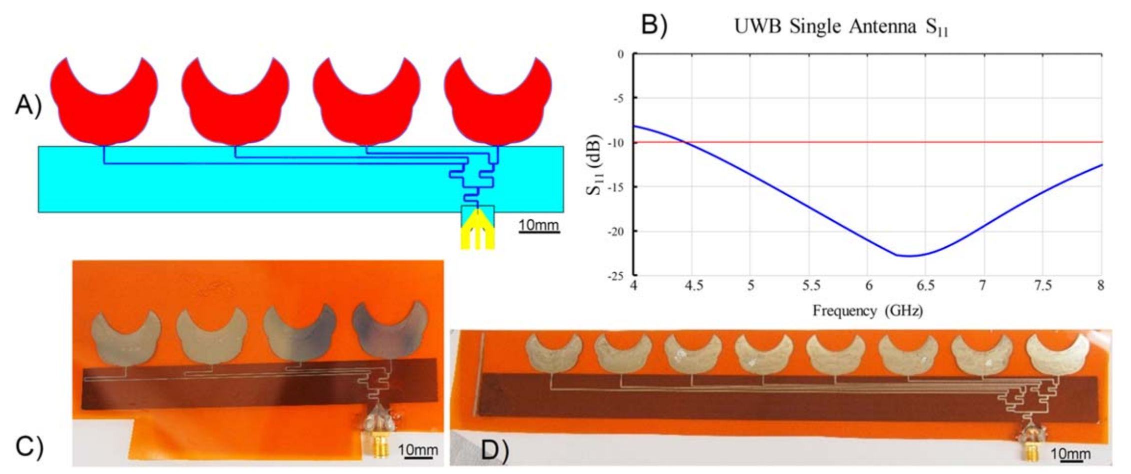

Figure 2. (A) Red is the antenna patch, dark blue the shifter network, yellow the SMA to microstrip transition, and cyan the backplane. The offset splitters minimizes the length of the microstrip lines. (B) S11 Performance of a single printed antenna. (C) A 1 × 4 array with an extended phase shifter. (D) A 1 × 8 array with a standard shifter.

attaching to PCBs and similar using off the shelf SMA hardware. To make up for the obvious differences in thickness, epoxy was used to both stabilize and provide a similar dielectric surface. This was then translated into a microstrip transmission line by creating an exponential taper that was mirrored on both the front plane and backplane, providing an impedance matched transition to the microstrip lines throughout the system [15, 16].

The shifter network was more difficult to design, due to the relatively high losses of microstrip lines on thin substrates [17, 18]. A power splitter design was used to maintain 50 Ohm impedance throughout the network, however it was found through simulation that the losses from unbalanced splitters was less than the longer microstrip transition lines [7]. Both the high loss of the microstrip lines and the unbalanced nature of the splitters was previously verified using Ansys simulation software [7]. These power splitters, used a gradual increase in width while moving through several corners to prevent sudden changes in impedance. Additionally, the corners were chamfered to control reflectance within the power splitters. This and the offset provided the fixed phase shifter portion of the system.

The key part of the design which enables the frequency scanning array capability is the broadband antenna patch. Many different broadband antenna patch designs have been demonstrated on printed substrates [5, 6, 19]. For this particular application, a stacked ellipsoid design was selected for its relatively compact size and known performance characteristics [7, 20]. Additionally, this particular antenna could be easily tuned to match the impedance of the shifter network without significant negative effects on the performance of the antenna. The S11 of this antenna is shown in figure 2(B).

2.3. Printing methodology

The frequency scanning arrays were all printed using a Dimatix DMP-2831 [21]. This printer is a maskless small scale 'drop on demand' type printer capable of printing feature sizes as small as 20 microns depending on the combination of inks and substrates being used. The substrate used was 5 mil Kapton Type HN, while the conductive traces were constructed using Novacentrix JS-B40G.

This class of drop on demand printer has significant limitations compared to state of the art systems in terms of resolution and throughput [22, 23]. However, it represents one of the best small scale ways to create prints capable of being reproduced on a roll-to-roll printer. Due to the fact that frequency scanning arrays only require conductive elements in their design, it is an ideal candidate for large scale production using roll-to-roll technology. Thus, a drop on demand printer was used as a proxy to demonstrate the potential for future large scale deployment.

125 micron thick kapton was first prepared by heat curing at 230 degrees C. These prepared sheets were then loaded into the Dimatix, and taped down to the platen. Novacentrix JS-B40G silver nanoparticle ink was loaded into the printer. The print was then completed with a drop spacing of 35 microns using the DXF files exported from Electronics Desktop. Five successive layers were printed on without curing, followed by a cure at 205 degrees C. This process was repeated for both the front and back of the substrate. An SMA connector was then attached to the input coupler using silver epoxy.

This design was fabricated in both a 1 × 4 and a 1 × 8 element configuration, and with both a shortest path phase shifter network as well as a network with an additional $\Delta\phi$ to increase the steerage per unit frequency. These devices were then tested to obtain far field radiation patterns, as well as performance under flex. Two of

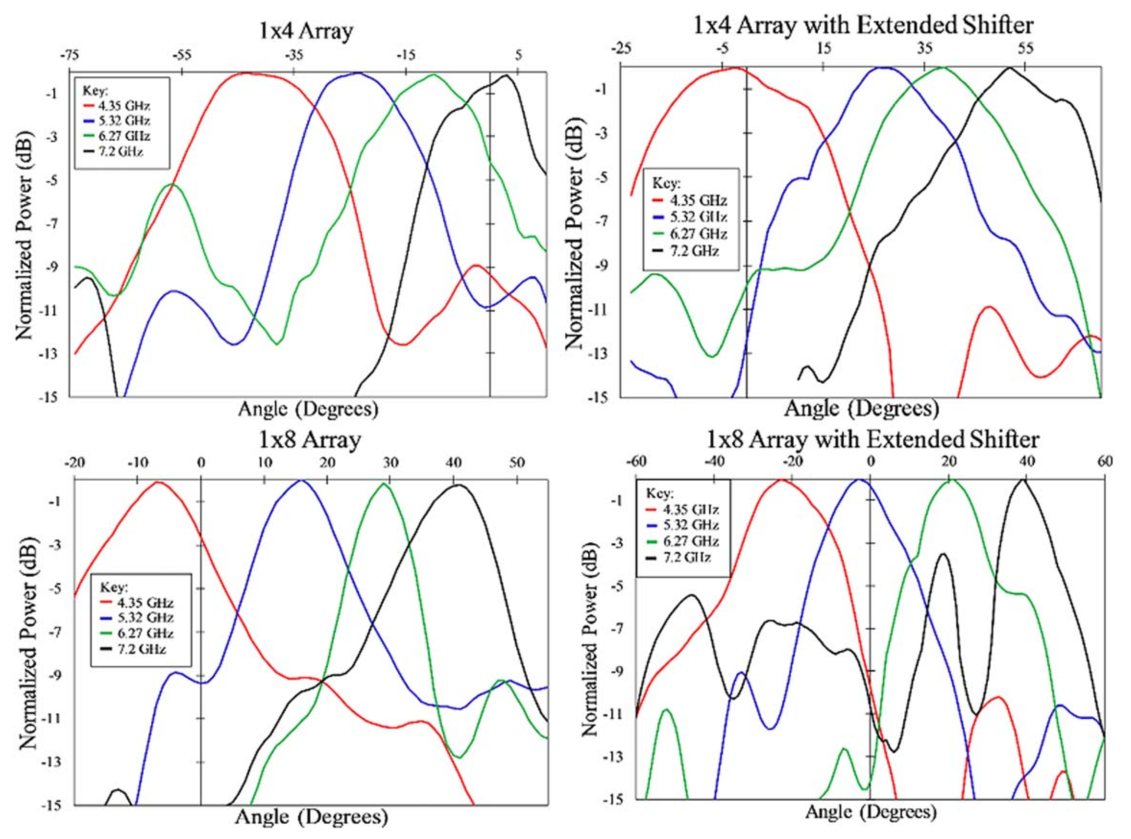

Figure 3. Extended shifter networks increase the swing per unit frequency, while the 8 element system exhibits narrower peak power.

the devices fabricated using these methods are shown in figure 2(C) and D. Both antenna arrays were 22 mm in height, while the 1 × 4 array was 122 mm in width and the 1 × 8 array was 250 mm in width. With the addition of the shifter and coupler, the total height of system was 45 mm for the 1 × 4 array and 55 mm for the 1 × 8 array. The width of the overall system depended on the particular phase shifter network, but was never more than 15 mm wider than the array.

2.4. Measurement methodology

Rotational measurements were made using a Microwave Spectrum Analyzer, high frequency signal generator, rotational stage and horn antenna. The FSA being tested was connected to the high frequency generator as a transmitting antenna, while the horn antenna was placed in the far field connected to the microwave spectrum analyzer. The frequency of the generator and MSA was then selected, and the rotational stage used to move through an entire 360 degree rotation recording the various values measured at each degree marker. These results were then collated and plotted.

S11 Results were obtained using an Agilent NS230A Network Analyzer. The antenna was directly connected to the Network analyzer output point to minimize system reflectance after calibrating.

3. Results

Beam steering was demonstrated across multiple devices, with steering per unit frequency varying depending on the number of elements on the array and the length of the phase shifters used. These results are shown in figure 3. Both 1 × 4 and 1 × 8 arrays with a shortest path and extended shifter network were tested in order to demonstrate the relationship between the length of the shifter network and the beam steering per unit frequency. Additionally, the two different sizes of arrays were tested to demonstrate the effect of greater elements on the steering phenomenology. Peak directional gain of the 1 × 4 array was observed at 12 dBi, and the 1 × 8 array was 15 dBi.

It is worth noting that for the physical devices, specific frequencies were tested, whereas for the previous work using simulation was able to do continuous peak capture to show the continuity of the illustrated shifting effect [7]. However, given the limitations of the measurement setup used for evaluating these devices, this was not possible. Consequently, the devices were each tested at a series of key frequencies to demonstrate the beam

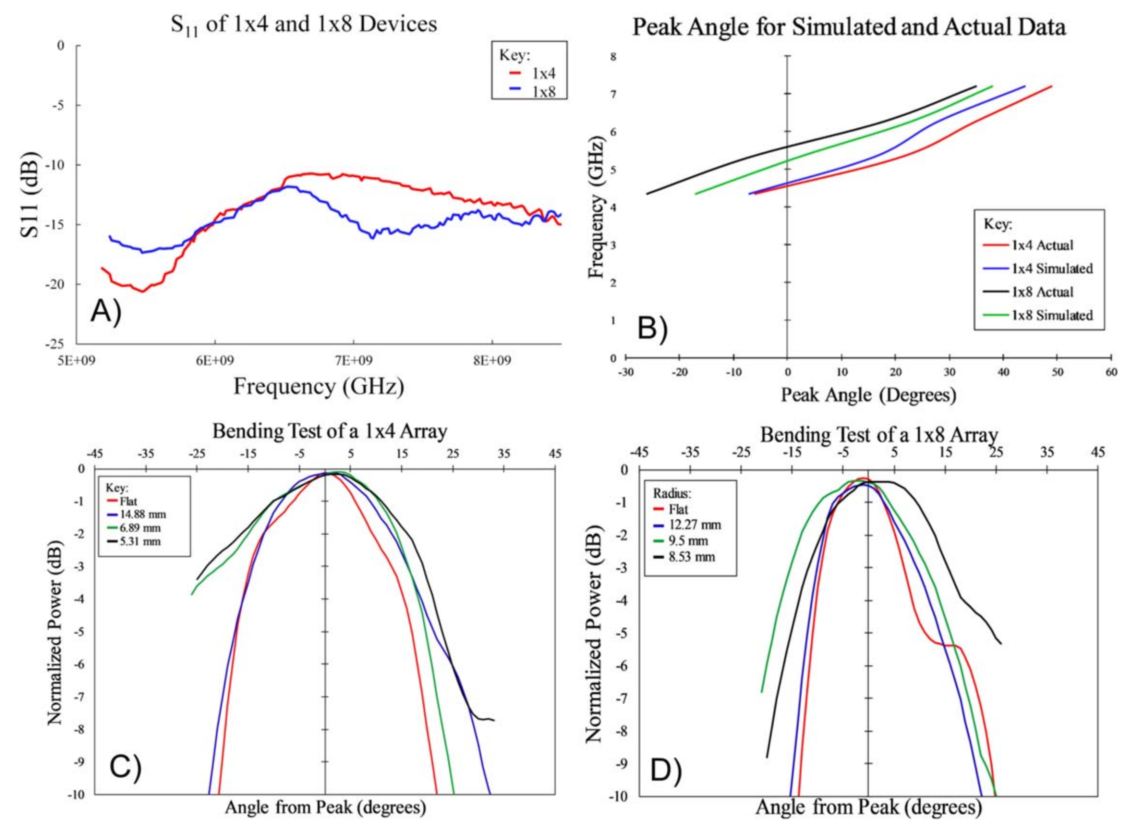

Figure 4. (A) The S11 of both the 1 × 4 and 1 × 8 devices shows less than 10 dB of reflection across the frequencies of interest. (B) The 1 × 4 and 1 × 8 devices show similar correlation between the actual measured and simulated results. (C) and (D) Both devices exhibited minimal distortion due to bending, but the 1 × 8 devices were more resilient due to their tighter beam.

steering and consistency with the simulated results. Based on the key frequency results and mathematical model of the frequency shifting, it can be concluded that the continuity in steering demonstrated in the simulations is also present in the physical devices.

S11 results, shown in figure 4(A), exhibited less than −10 dB of reflectance across the entire range of interest for both the 1 × 4 and 1 × 8 devices. The 1 × 8 device showed less reflectance from 6.5 to 7.5 GHz, which corresponds to inefficiencies in the longer transmission lines and additional power splitters leading to larger losses. Radiation efficiency at peak transmitivity for the 1 × 4 devices was observed to be 23%, while the 1 × 8 devices exhibited similar peak numbers but showed more significant drop off in efficiency as the frequency increased. This caused the development of a much larger side lobe for the 1 × 8 extended shifter at 7.2 GHz, as the signal strength was lower and the radiation efficiency was also reduced, leading to a much smaller gain relative to the side lobes.

In addition to the rotational measurements, bending tests were also done. Given the potential for flexible electronics devices built using inkjet deposition, it is essential to understand what performance is like under these scenarios. The results of these tests are shown in figures 4(C) and (D).

Given the minimal loss of performance under bending tests, the Frequency Scanning Array is an ideal type of antenna to be used in situations where both spatial signals and directionality are needed. Many flexible substrate devices exhibit significant losses in performance under bending tests. However, due to the fact that FSA results are assessed from the far field, the bending required to show performance loss is relatively extreme. Combined with the low cost to manufacture, these devices represent an immediate potential application for flexible printed electronics.

4. Discussion

The first point in interpreting the results is to ensure that they make sense from a physics standpoint. Beyond the equations outlined in this paper, the peak values were compared to previously simulated results [7]. The extended shifters were used for comparison as these are the more interesting devices performance wise, with the results summarized in figure 4(B).

Note that both devices show stronger correlation on one end of the range than the other. This is due to differences in the slope or change per unit frequency for the simulated vs actual devices. This difference can be accounted for given the dimensional inaccuracies of the Dimatix system. The simulation is based off the designed dimensions, such as microstrip transmission lines with a width of 285 microns, whereas the actual results were closer to 310 microns. This can cause significant changes in the S11 performance of several of the components in the system.

There are several different elements in the measured results that warrant further discussion. First and foremost is the basic properties stemming from the steerability as a function of frequency. While this has been demonstrated previously using rigid array antennas [24], these devices have not been built using inkjet deposition technologies. Thus, we must first consider the basic capabilities of the array.

Both the 1×4 and 1×8 arrays exhibit typical array antenna properties and similar levels of gain. The 1×8 arrays have a much narrower −10 dB gain angle than the 1×4 devices, which is generally the goal in increasing the number of elements in an array. Changing the number of elements in the array also shifts the center of the angle range encompassed by the 4 different frequencies tested for these antennas. This is product of the shifts in the S11 caused by introducing additional power splitters in the design. Note however that increasing the number of elements does not significantly alter the shift per unit frequency. This implies that higher element count antennas would show similar steering characteristics independent of the element count.

Additionally, increasing the length of the fixed phase shifter path increases the amount of steering exhibited per unit frequency. This is expected based on the equation governing the angle of transmission as a function of frequency. This effect is somewhat independent of the number of elements in the array, as both the 1×4 and 1×8 arrays have a similar total swing in angle. However, while the total swing was similar across frequencies, the distance between the intervening peaks varied. This speaks to the difficulty in designing these types of antenna arrays. The S11 of the patch antenna, power splitter, coupler, and microstrip lines all interact to produce the final signal. This means the simple addition of a power splitter or longer transmission line significantly shifts the center frequency of an antenna array. Designing to these specifications without the usage of EM software such as Ansys Electromagnetics would be very difficult.

Given the fact that these devices were produced on flexible substrates, it is also important to consider the performance under the bending test. The usage of 5 mil Kapton HN provides excellent tensile performance compared to other polymide films [13], and the usage of a silver/polymer nanocomposite ink further improves lifetime flex performance of the devices as has been demonstrated in other papers [25]. Both the 1×4 and 1×8 devices presented usable performance under bending. However, the 1×8 was more resilient, showing adequate performance through all the tested values. In contrast the 1×4 devices began to degrade significantly around a 10mm radius. This test implies that denser arrays with more elements will be better for flexible electronics applications.

Note that denser arrays with more elements will incur an additional cost in producing these devices, as it will require both additional print time and materials. These negative effects can be combatted through the usage of small area fractal antennas [26] but fundamentally dense arrays will always cost more than their less dense counterparts. Optimization of the cost performance curve should be done on a per application basis, as dense array performance may not be needed in certain applications, while high flex applications may make it a necessity.

5. Conclusion

Due to the usage of only conductive inks in the production of the frequency scanning arrays, these can be easily printed with very high yield rates. Thus, this represents a printed device which can be mass produced using currently available printing technologies. Performance was shown to be adequate in flexible conditions to consider using this in applications where significant active bending was likely to occur. This combined with the simultaneous receiving capability inherent in these technologies creates a compelling argument for building these devices for communications applications with a location component.

Future work should focus on improving performance of microstrip transmission lines to limit loss and shrink the overall package of the device. This could be accomplished via the usage of dimensionally smaller broadband antennas. Additional work into alternate phase delay structures could also yield promising gains.

Acknowledgments

Research was funded through the University of Texas at Austin. Special thanks to Travis Lenz and Farzad Mokhtari-Koushyar for assistance provided in running the printing systems.

ORCID iDs

Peter Mack Grubb https://orcid.org/0000-0002-1405-7564

References

[1] Weisbecker A, Burmester M and Schmidt A 2015 *Mensch und Computer 2015—Workshopband.* (Germany: de Gruyter) 978-3-11-044390-5

[2] Subbaraman H *et al* 2013 Inkjet-printed two-dimensional phased-array antenna on a flexible substrate *Antennas Wirel. Propag. Lett. IEEE* **12** 170–3

[3] Grubb P M *et al* 2016 X-band printed phased array antennas using high-performance CNT/ion gel/Ag transistors *Proc. SPIE* **9738** 973813

[4] Byun K, Subbaraman H, Lin X, Xu X and Chen R T 2013 A 3 μm channel, ink-jet printed CNT-TFT for phased array antenna applications *in Wireless and Microwave Circuits and Systems (WMCS), 2013 Texas Symp. on* pp. 1–3

[5] Chen Z N, See T S P and Qing X 2007 Small printed ultrawideband antenna with reduced ground plane effect *IEEE Trans. Antennas Propag.* **55** 383–8

[6] Casula G A, Montisci G and Mazzarella G 2013 A wideband PET inkjet-printed antenna for UHF RFID *IEEE Antennas Wirel. Propag. Lett.* **12** 1400–3

[7] Grubb P M, Li W, Mokhtari-Koushyar F and Chen R T 2018 All inkjet printed frequency steered phased array antennas with multi angle receiving demonstrated via simulation *Laser 3D Manufacturing V* **10523** 105230T

[8] Garakoui S K, Klumperink E A M, Nauta B and van Vliet F E 2011 Phased-array antenna beam squinting related to frequency dependency of delay circuits *41st European Microwave Conference* pp. 1304–7

[9] Hall P S and Vetterlein S J 1990 Review of radio frequency beamforming techniques for scanned and multiple beam antennas *IEE Proc. H Microw. Antennas Propag.* **137** 293–303

[10] Hansen R C 2009 *Phased Array Antennas.* (New York: Wiley)

[11] Mailloux R J 2005 *Phased Array Antenna Handbook* vol 2 (Boston: Artech House)

[12] Weinstein S and Ebert P 1971 Data transmission by frequency-division multiplexing using the discrete fourier transform *IEEE Trans. Commun. Technol.* **19** 628–34

[13] 2014 Dupont.com, 'KAPTON POLYMIDE FILM' [Accessed 14-Jun-2018] http://www.dupont.com/products-and-services/membranes-films/polyimide-films/brands/kapton-polyimide-film.html

[14] Zardetto V, Brown T M, Reale A and Di Carlo A 2011 Substrates for flexible electronics: a practical investigation on the electrical, film flexibility, optical, temperature, and solvent resistance properties *J. Polym. Sci. Part B Polym. Phys.* **49** 638–48

[15] Xia T, Yang S and Nie Z 2009 'Design of a tapered balun for broadband arrays with closely spaced elements *IEEE Antennas Wirel. Propag. Lett.* **8** 1291–4

[16] Tapered Transitions [Accessed: 13-Jul-2016] http://www.sigcon.com/Pubs/edn/TaperedTransitions.htm

[17] Garg R, Bahl I and Bozzi M 2013 *Microstrip Lines and Slotlines* Third Edition (Boston: Artech House) 9781608075355

[18] Coonrod J and Rautio B 2012 Comparing microstrip and CPW performance *Microw. J.* **55** 74–86

[19] Cook B S and Shamim A 2013 Utilizing wideband AMC structures for high-gain inkjet-printed antennas on lossy paper substrate *IEEE Antennas Wirel. Propag. Lett.* **12** 76–9

[20] Schulz C, Baer C, Musch T and Rolfes I 2011 A broadband stacked patch antenna with enhanced antenna gain by an optimized ellipsoidal reflector for X-band applications *IEEE International Conference on Microwaves, Communications, Antennas and Electronic Systems (COMCAS 2011)* pp. 1–7

[21] Dimatix Materials Printer DMP-2831 | Deposition Products | Industrial Inkjet Printheads | Fujifilm USA. [Accessed: 06-May-2015] http://fujifilmusa.com/products/industrial_inkjet_printheads/deposition-products/dmp-2800/

[22] Optomec, 'Aerosol Jet' [Accessed: 18-Jun-2018] https://www.optomec.com/printed-electronics/aerosol-jet-technology/

[23] Grau G and Subramanian V 2016 Fully high-speed gravure printed, low-variability, high-performance organic polymer transistors with Sub-5 V operation *Adv. Electron. Mater.* **2** n/a-n/a

[24] Frankel M Y and Esman R D 1995 True time-delay fiber-optic control of an ultrawideband array transmitter/receiver with multibeam capability *IEEE Trans. Microw. Theory Tech.* **43** 2387–2394

[25] Lee H-H, Chou K-S and Huang K-C 2005 Inkjet printing of nanosized silver colloids *Nanotechnology* **16** 2436

[26] Maza A R, Cook B, Jabbour G and Shamim A 2012 Paper-based inkjet-printed ultra-wideband fractal antennas *Antennas Propag. IET Microw.* **6** 1366–1373